Polish J. Chem., **76**, 1467–1480 (2002)

Equilibrium Isotope Effects on the Crotonase Reaction

by M. Kołodziejska-Huben[1], V.E. Anderson[2] and P. Paneth[1*]

[1]*Institute of Applied Radiation Chemistry, Technical University of Łódź, Żeromskiego 116, 90-924 Łódź, Poland*
[2]*Department of Biochemistry, Case Western Reserve University, 10900 Euclid Avenue, Cleveland, Ohio 44106, USA*

(Received April 2nd, 2002; revised manuscript June 14th, 2002)

Equilibrium isotope effects on the enoyl-CoA hydratase (crotonase, ECH) – catalyzed reaction were modeled by a mixed QM/MM method. The classical region (27 aminoacids essential for the catalysis) was treated at the MM level using universal force field UFF. The quantum atoms of 4-(*N,N*-dimethylamino)cinnamoyl-CoA (DAC-CoA), one water molecule, and two glutamate residues (Glu164 and Glu144) in the active site were treated at the PM3 level.

Key words: enoyl-CoA hydratase, equilibrium isotope effect, QM/MM method, CM2

Understanding the catalytic power of enzymes is essential, because of their central role in all chemical processes in living systems. Understanding enzyme mechanisms provides a key to drug design, use of enzymes for synthesis, design of altered enzymes, among other uses. Isotope effects are particularly suited for detailed studies of the nature and relative rates of chemical events within an enzyme active site and details of its catalytic action.

Theoretical predictions are of special value in relation to the systems, where the experimentally determined value of an isotope effect is not intuitively attributable to a particular mechanism. This type of computational experiment requires a method that is known to accurately reproduce molecular properties of substrates and products (if an equilibrium isotope effect is being calculated) or substrates and corresponding transition states (for kinetic isotope effect calculations).

Enoyl-CoA hydratase (crotonase) catalyzes addition of water molecule to 4-(*N,N*-dimethylamino)cinnamoyl-CoA (DAC-CoA) yielding propenoyl thiolester (Fig. 1).

Enoyl-CoA hydratase catalyzes the *syn* addition of a water molecule across the double bond of a range of *trans*-2-enoyl-CoA derivatives [1]. On the basis of thorough isotope effect studies [2,3], it was proposed that crotonase catalyzes a concerted reaction, where both the C–H and C–O bonds are formed in a single transition state. An activated water molecule acts as the nucleophile in this mechanism. This would require an activated Michael acceptor, suggesting the possibility that the crotonase active site would induce a polarization of the carbon-carbon double bond of the sub-

*Corresponding author.

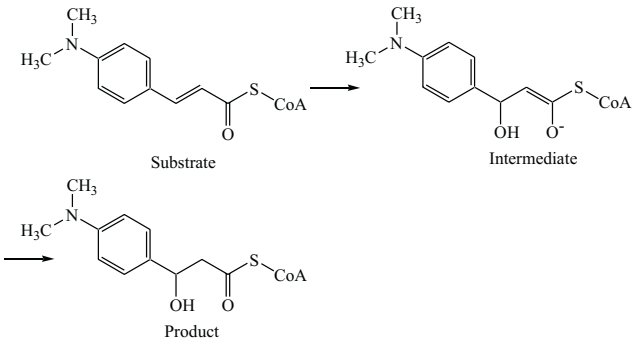

Figure 1. Structures of substrate, intermediate and product.

strate. However, on the basis of β-secondary deuterium isotope effect [4,5] a stepwise reaction was postulated.

The environment of ligand's potential hydrogen bond donors or acceptors changes dramatically upon transfer from the aqueous solution to the enzyme active site. These changes may be manifested in the altered vibrational frequencies of bonds participating in binding. This should cause small but measurable isotope effects on binding.

In this paper we present results of the calculations of the equilibrium isotope effects on the crotonase catalyzed reaction in order to put some light into effects caused by the active site of the enzyme.

COMPUTATIONAL DETAILS

Reactant. DAC-CoA in the aqueous solution was optimized using the PM3 Hamiltonian [6,7] and explicit water model. In the first step of constructing the water model DAC-CoA was "soaked" in the TIP3P [8] water box (23.1:24.4:24.7 Å:Å:Å) containing 246 molecules of water. Then all water molecules, which were outside the 8 Å radius from the carbonyl oxygen of DAC-CoA, have been discarded. The radius selected corresponds to the one, used for the construction of the active site model (see below). The geometry of DAC-CoA is very non-spherical. If all water molecules around it were kept in the model, the number of degrees of freedom increases significantly with many water molecules far away from the center of the reaction. However, when only water molecules within the 8 Å radius are present, significant

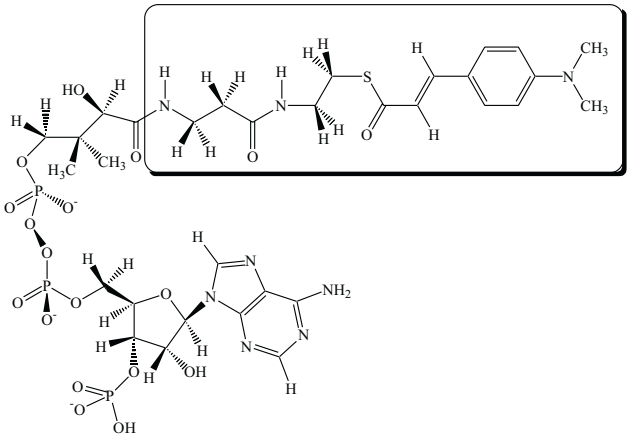

Figure 2. Structure of DAC-CoA with frame around the part used in calculations.

part of the reactant remains unsolvated. We have, therefore, decided to truncate the model of the reactant. The part sticking out from the solvation sphere was removed. Fig. 2 illustrates the selection made. Atoms outside the frame were removed and a hydrogen atom was added to the nitrogen involved in the amide bond along which the truncation was made.

The model constructed in this way consisted of 67 water molecules and DAC-CoA (246 atoms). It was optimized initially in Hyperchem ver. 5.1 [9] to the gradient of 0.0007 kcal/mol/Å and subsequently reoptimized* in Gaussian [10] to the gradient of 0.07 kcal/mol/Å. The structure of the optimized model is shown in Fig. 3.

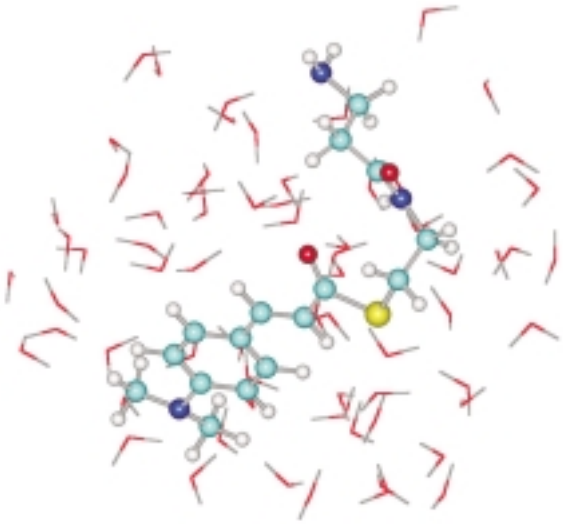

Figure 3. Optimized structure of the aqueous solution model. Water molecules rendered with sticks for clarity.

The same method was used for the optimization of the product in the aqueous solution using explicit water model. Model of the product in the aqueous solution was created from the model of the substrate in the aqueous solution described above. The product is an adduct of a water molecule to the double bond C_3=C_4 of DAC-CoA (numbering of atoms is given in Fig. 4). The necessary changes were included manually by addition of OH groups of the nearby water molecule to the C_4 atom and the H atom of the same water molecule to the C_3 atom of DAC-CoA. The model constructed in this way consisted of 66 water molecules and propenoyl thiolester (246 atoms). It was optimized in Gaussian to the gradient of 0.0035 kcal/mol/Å.

Enzyme active site was modeled using mixed QM/MM method within the ONIOM [11–15] scheme as implemented in the Gaussian package. Initial coordinates were taken from the crystallographic data of the enoyl-CoA hydratase catalytic hexamer obtained from the PDB (file 2DUB.pdb). The model included aminoacids within the 8 Å radius from the carbonyl oxygen of DAC-CoA. Where necessary the N-terminal ends of aminoacids were capped with hydrogen atoms to form $–NH_2$, and the C-terminal ends

*Hyperchem uses only gradient criteria for the termination of an optimization, while Gaussian uses additionally geometric criteria. The program we have used for calculations of isotope effects, Isoeff98, requires full Hessian matrix in the Cartesian space, which is not available from Hyperchem output. Initial model building and optimization was thus carried out in Hyperchem taking advantage of the convenience of its GUI. However, the final calculations of Hessian had to be carried out using Gaussian. We have noticed that when very tight convergence criteria are used in Hyperchem optimization the convergence of the additional Gaussian criteria can be achieved within a few cycles. This is especially important in the present case, where 67 individual water molecules are used and the energy surface is very flat.

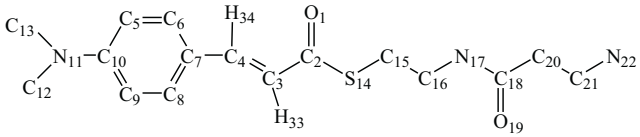

Figure 4. Numbering of atoms in the model of the reactant.

were capped by amino groups to form $–CONH_2$. DAC-CoA model was truncated as described above (Fig. 2). The net charge of –2 was assigned to the model on the basis of the expected protonation state of the aminoacids at the physiological pH. The model created in this way includes 480 atoms. Out of this number 82 atoms including DAC-CoA, one water molecule, and two aminoacids: Glu-144 (charge –1) and Glu-164 (charge 0) were treated quantum mechanically using the semi-empirical PM3 Hamiltonian. The remaining part of the model of the enzyme active site was treated at the molecular mechanics level using the universal force field UFF [16,17]. The division between the QM and MM regions includes three amide bonds between Glu144 and Leu145 and Cys143, and between Glu164 and Pro163. Hydrogen atoms were added to satisfy the valence of the QM fragment. Fig. 5 shows model of the reactant in the active site of the enzyme.

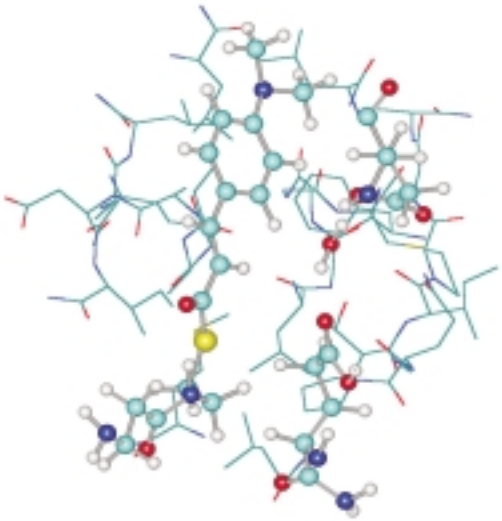

Figure 5. Model of the ECH active site with bounded DAC-CoA used in the QM/MM calculations. Active site residues rendered with sticks for clarity.

Model of the product in the ECH active site was created from the model of the ECH active site with bounded DAC-CoA described above in the same way as model of the product in the aqueous solution. The structure was then reoptimized. The model prepared in this way includes the same number of atoms as the model of the reactant in the active site and also division into QM and MM layers is the same. The model of the enolate intermediate in the active site was generated from model of the product in the active site by transferring the proton from C_3 to Glu 164. The model was optimized in Gaussian to the gradient of 0.0225 kcal/mol/Å.

Hessian calculations were performed for all optimized structures to ensure that they represent stationary points and for the calculations of isotope effects.

Equilibrium isotope effects were calculated from [18]:

$$\frac{K_{16}}{K_{18}} = \prod_{i}^{3n-6} \frac{u^{P}_{i(L)}}{u^{P}_{i(H)}} \frac{\sinh \frac{1}{2} u^{P}_{i(H)}}{\sinh \frac{1}{2} u^{P}_{i(L)}} \prod_{i}^{3n-6} \frac{u^{S}_{i(H)}}{u^{S}_{i(L)}} \frac{\sinh \frac{1}{2} u^{S}_{i(L)}}{\sinh \frac{1}{2} u^{S}_{i(H)}} \tag{1}$$

where K_{16}/K_{18} is the calculated equilibrium isotope effect, n is the number of atoms in the molecule, $u_i = h\nu_i/\mathbf{k}T$, where h and **k** are Planck and Boltzmann constants, respectively, T is the absolute temperature and ν_i are the frequencies of normal modes of vibrations. Subscripts "16" and "18" correspond to ^{16}O or ^{18}O substituted species, respectively, while the "S" and "P" superscripts indicate the properties of the substrate or product molecules. Isotope effects were calculated using the Isoeff98 program [19].

RESULTS AND DISCUSSION

Isotope effects are very useful in learning details of chemical and enzymatic reactions. We have shown previously experimentally and theoretically that equilibrium ^{18}O isotope effects on association of oxamate with lactate dehydrogenase in the presence of the cofactor, NADH, can provide information on the binding of a reactant to an enzyme [20,21]. The equilibrium ^{18}O isotope effect for carboxylic oxygen has been found to be 0.9840 by the equilibrium dialysis. Significantly inverse value of the equilibrium ^{18}O isotope effect was ascribed to the formation of bifurcated hydrogen bonds upon binding. Theoretical MO calculations allowed the quantification of the observed value in terms of the rearrangement of the hydrogen bonding network around the isotopic atom. We were interested in the equilibrium ^{18}O isotope effects on the crotonase reactions because the value of this effect can provide information about the hydrogen bond strength. Measurement of isotope effects on formation of enzyme-ligand for large number of systems could result in correlation of EIE's with the strength of individual hydrogen bonds and has potential application in the design of enzyme inhibitors.

One clear difference between enzyme catalysis and solution reactions is ordered arrangement of electrostatic charges at the active site that serves as a specific "solvation field" for the reactants and transition states. This problem has been addressed theoretically but experimentally demonstrating the strength of "electrostatic solvation" is a difficult undertaking. Our calculations aim at explanation and quantification of the electronic alteration of reactants in the active site of the enzyme.

Using our model described above, we have found that a water molecule in the model with substrate bound to the enzyme is hydrogen bonded between the two catalytic glutamate residues, Glu144 and Glu164 and the lengths of these bonds are 1.74 Å and 1.86 Å, respectively (Fig. 6). Glu144 is in position to facilitate the addition of water to the C_4 carbon of the substrate. The distance between oxygen of the water molecule and carbon atoms C_3, C_4 of the substrate is 3.8 Å and 3.6 Å, respectively. The carbonyl oxygen hydrogen-bonded with two amide protons from Ala 98 and Gly141 forms an "oxyanion hole". Similar structure has been observed in serine proteases [22,23]. The optimized hydrogen bond distances between the atoms at the active site are summarized in Table 1.

Table 1. Hydrogen bond distances (Å) in the structures of reactant and product optimized in the active site.

residue	substrate	product
Glu 144	1.74 (H_W-O_{Glu})[a]	2.80 (O_{46}-H_{Glu})
Glu 164	1.86 (H_W-O_{Glu})	1.83 (H_{47}-O_{Glu})
Ala 98	2.45(H_{Ala}-O_1)	–
Gly 141	2.50(H_{Gly}-O_1)	–

[a]H_W, H_{Ala}, H_{Gly}, H_{Glu} correspond to hydrogen in the water molecule, hydrogen in –NH group in alanine, and glycine, and hydrogen in –COOH group in glutamate, respectively. O_{Glu} corresponds to the oxygen in glutamate. For the definitions of O_{46}, H_{47} see Fig. 8.

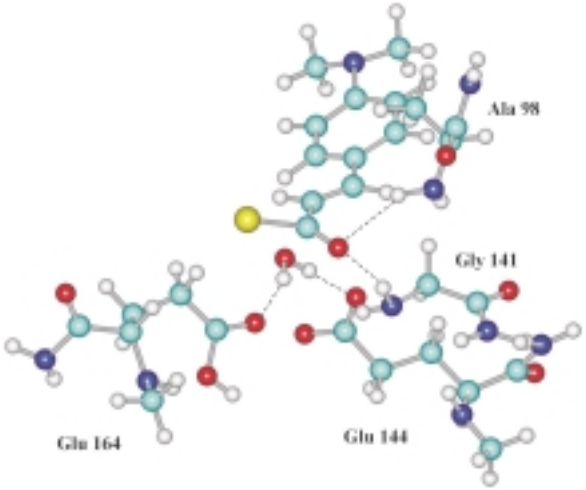

Figure 6. Optimized structure of the substrate in the active site. DAC-CoA was truncated at the sulfur atom for clarity.

The optimized structure of the intermediate in the active site shows that Glu164 and Ala98 form hydrogen bonds with the intermediate (Fig. 7).

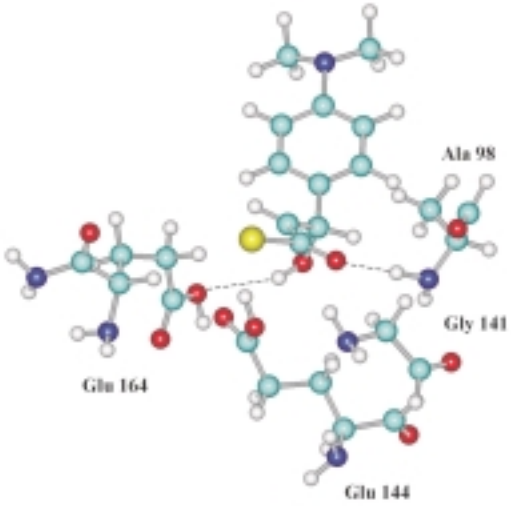

Figure 7. Optimized structure of the intermediate in the active site. DAC-CoA was truncated at the sulfur atom for clarity.

The optimized structure of the product in the active site shows that Glu144 and Glu164 form hydrogen bonds with the product (Fig. 8).

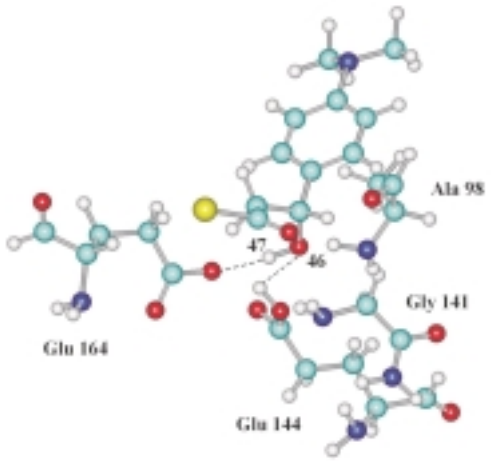

Figure 8. Optimized structure of the product in the active site. DAC-CoA was truncated at the sulfur atom for clarity.

Distances between O_1 and nitrogen atoms of Ala 98 and Gly141 suggest that the enolate intermediate is stabilized in the enzyme active site (Table 2). Our results are in agreement with those postulated by Anderson (unpublished data).

Table 2. Distances (Å) between O_1 and N from residues in the structures of substrate, intermediate and product optimized in the active site.

residue	substrate	intermediate	product
Gly 141	3.52	2.86	3.16
Ala 98	3.27	3.23	3.18

We have studied changes in the ground state electron distribution upon binding using the PM3 method and CM2 partial atomic charges as implemented in Amsol6.6 [24]. The largest changes between the substrate in the aqueous solution and in the active site are observed for the double bond C_3=C_4 (charge on the atom C_3 decreased by 0.09, while on the atom C_4 increased by 0.09) and C_2=O_1 (charge on the O_1 decreased by 0.07, while on the C_2 increased by 0.03). Thus crotonase active site polarizes the double bond between C_3 and C_4 of the substrate and enhances the electrophilicity of the β carbon. Changes in charge distribution in case of the aromatic ring are not significant (partial charge on atoms C_6, C_8, C_9, C_{10} increases by 0.01, 0.04, 0.01 and 0.01, respectively, and on atoms C_5 and C_7 decrease by 0.01). The charge on the atom N_{11} changes by only 0.02. The results obtained by the CM2 method differ quantitatively and qualitatively from those obtained by the Mulliken analysis. The largest changes between the substrate in the active site and intermediate in the active site are observed

Table 3. Calculated partial atomic charges.

atoms	substrate in aqueous solution		substrate in the active site		intermediate		product in the active site		product in aqueous solution	
	CM2	Mulliken	CM2	Mulliken	CM2	Mulliken	CM2	Mulliken	CM2	Mulliken
O_1	–0.44	–0.34	–0.51	–0.32	–0.60	–0.49	–0.46	–0.34	–0.41	–0.30
C_2	0.48	0.29	0.51	0.28	0.52	0.34	0.46	0.27	0.44	0.24
$C_3(C_\alpha)$	–0.29	–0.15	–0.38	–0.14	–0.62	–0.62	–0.32	0.00	–0.19	–0.01
$C_4(C_\beta)$	0.05	0.17	0.14	0.12	0.28	0.25	0.19	0.23	0.20	0.23
C_5	–0.16	–0.04	–0.17	–0.07	–0.16	–0.16	–0.16	–0.06	–0.15	–0.03
C_6	–0.04	0.07	–0.03	0.07	–0.07	–0.07	–0.06	0.04	–0.05	0.08
C_7	–0.15	–0.17	–0.16	–0.13	–0.09	–0.09	–0.14	–0.13	–0.17	–0.19
C_8	–0.05	0.07	–0.01	0.14	–0.08	–0.08	–0.07	0.07	–0.07	0.06
C_9	–0.18	–0.04	–0.17	–0.04	–0.17	–0.17	–0.16	–0.04	–0.17	–0.04
C_{10}	0.14	0.01	0.15	0.00	0.09	–0.05	0.11	–0.05	0.09	–0.06
N_{11}	–0.39	0.01	–0.37	0.00	–0.40	0.02	–0.39	0.00	–0.40	–0.01
C_{12}	0.02	0.06	–0.01	0.04	0.01	–0.12	0.00	0.03	–0.01	0.04
C_{13}	0.02	0.06	0.00	0.04	0.00	–0.12	0.00	0.02	0.02	0.05
S_{14}	–0.23	–0.08	–0.23	–0.06	–0.41	–0.25	–0.24	–0.07	–0.23	–0.08
C_{15}	–0.13	0.02	–0.14	–0.04	–0.14	–0.22	–0.13	–0.03	–0.11	0.01

for C_3, S_{14}, O_1, C_8, C_6, C_{10} (charge decreased by 0.24, 0.18, 0.09, 0.07, 0.06 and 0.04, respectively) and C_4, C_7 (charge increased by 0.14, 0.07, respectively) (Table 3).

Mulliken charge distribution shows the largest changes in the aromatic ring indicating polarization of only in this ring. The largest changes are observed for C_5 (charge decreased by 0.03), C_7 (increased by 0.04), and C_8 (increased by 0.07). The charge on the atom C_4 decreases by 0.05, while CM2 method gives an increase by 0.09. When we compare substrate in the active site with the intermediate in the active site, we observe changes in the Mulliken charge distribution for all atoms. Charges decreased on the atoms C_3, C_8, S_{14}, C_{15}, O_1, $C_{12,}$ C_{13}, C_9, C_5, and C_{10} by 0.48, 0.22, 0.19, 0.18, 0.17, 0.16, 0.16, 0.13, 0.09, and 0.05, respectively. On the atoms C_4, C_2 and C_7 charge increased by 0.13, 0.06, and 0.04, respectively. Mulliken analysis was the base of the discussion presented by Carey *et al*. [25], which led to the conclusion that the major electronic changes upon binding occur in the ring. Since CM2 charges provide better description of these changes we believe that the polarization induced by crotonase affects mostly the double bond. It is worth noticing that our results provide an example of the qualitatively different interpretation of the enzyme action upon using more realistic atomic charge scheme. They also stress the importance of using realiable schemes and provide warning for drawing conclusions from widely used, but very simple Mulliken population analysis.

The C_2=O_1 bond length is shorter by 0.005 Å, C_3=C_4 by 0.003 Å, C_2–C_3 by 0.01 Å, C_{14}–C_{15} by 0.01 Å and C_{21}–N_{22} by 0.01 Å for bound substrate than for free substrate. The C_4–H_{34} bond distance changed from 1.100 Å (substrate in aqueous solution) to 1.097 Å (substrate in the active site). The C_3–H_{33} bond length is larger by 0.003 Å, C_4–C_7 by 0.001 Å, and C_2–S_{14} by 0.01 Å for bound substrate than for free substrate. The C_{10}–N_{11} bond distance changed from 1.143 Å (substrate in aqueous solution) to 1.443 Å (substrate in the active site). The remaining bonds are intact. In Table 4 selected dihedral angles are summarized. The dihedral angle C_8–C_7–C_4–C_3 in free substrate is close to zero. Crystallographic data for the bound substrate showed that the aromatic ring is twisted along double bond C_3=C_4 axis. In agreement with these finding our calculations indicate that the value of dihedral angle C_8–C_7–C_4–C_3 in enzyme-bound substrate is 13.7°. As stated above, major π-electron reorganization occurs for the C_2=O_1 and C_3=C_4. This is reflected in the vibrational character of the enzyme-bound substrate. The mode near 1913 cm^{-1} for substrate in aqueous solution is associated with carbonyl group. One band 1923.7 cm^{-1} is observed for carbonyl group in substrate in the active site (Table 5). The band 1827.6 cm^{-1} due to the double bond C_3=C_4 (substrate in aqueous solution) is shifted to 1825.2 cm^{-1} (substrate in the active site). The key aromatic ring mode near 1551 cm^{-1} for the free substrate remains "intact" for the bound form. The bands 1215.4 and 1263.4 cm^{-1} (substrate in aqueous solution) for the aromatic ring are moved to 1194.5 and 1259.5 cm^{-1} (substrate in the active site), respectively.

Table 4. Selected dihedral angles.

dihedral angle	substrate in aqueous solution	substrate in active site	enolate intermediate	product in active site	product in aqueous solution
C_{11}–C_{10}–C_5–C_6	174.8	171.7	175.3	175.6	–177.9
C_8–C_7–C_4–C_3	0.6	13.7	–53.3	53.9	–60.2
C_7–C_4–C_3–C_2	–179.8	–174.7	–139.9	–130.8	–167.2
C_4–C_3–C_2–S_{14}	–179.8	156.1	–171.6	178.5	–163.9
C_2–S_{14}–C_{15}–C_{16}	–88.2	–57.3	–110.3	–101.3	–86.3
S_{14}–C_{15}–C_{16}–N_{17}	87.4	99.6	135.5	137.1	117.6
C_{15}–C_{16}–N_{17}–C_{18}	78.2	76.0	105.6	70.4	72.9
C_{16}–N_{17}–C_{18}–C_{20}	–166.8	–177.4	–159.9	–170.6	–168.9
N_{17}–C_{18}–C_{20}–C_{21}	–84.1	–139.1	–139.9	–110.0	–138.4

Table 5. Calculated frequencies for substrate in aqueous solution and substrate in the active site, ν (cm^{-1}).

substrate in aqueous solution	substrate in the active site	modes
383.7	–	ring
386.1	–	ring
396.5	392.0	ring
426.3	415.8	ring, C_3=C_4
438.3	443.5	ring, S–C–O, C_3=C_4
451.3	–	ring
469.5	479.1	ring, C=O
501.6	505.7	ring, S–C–O
–	514.7	CH_3
556.6	554.4	ring, N–CH_3
571.9	–	ring
592.6	–	ring
607.6	620.1	ring, C–S
619.9	–	C–S, C=O, ring
635.5	653.7	ring, C–S
645.5	–	C–S
661.6	–	ring
–	702.9	ring, C–S–O, C=O
754.5	739.1	ring, C–S–O, C=O
–	811.2	ring, C–S
819.9	882.3	ring, C–S, N–CH_3
–	931.6	ring, C–H
945.1	945.4	ring, C_3=C_4, CH_3
–	981.9	ring
1019.3	–	ring C–H
1033.3	1032.9	CH_2, CH_3
–	1034.0	CH_2
1054.2	1052.8	CH_3, ring
1098.4	1152.9	ring, C–H
1171.2	–	N–CH_3
–	1159.5	CH_2
1215.4	1194.5	ring C–H, N–CH_3
1246.7	1245.6	ring C–H
1263.4	1259.5	ring, C_3=C_4
–	1277.7	CH_2
1329.5	1303.8	ring C–H, N–CH_3
1360.2	1340.6	ring C–H, CH_3
–	1352.3	ring C–H
1368.4	1368.8	CH_2, CH_3
1377.7	–	CH_2
1396.5	1392.3	CH_2
–	1401.6	CH_3
1430.9	–	CH_2
1479.3	1447.2	ring C–H

Table 5 (continuation)

–	1499.9	CH_2
1501.3	1517.3	ring C–H
1551.2	1551.6	ring
1632.8	1640.3	ring C–H
–	1760.9	ring C–H
1827.6	1825.2	C_3=C_4
1913.8	1923.7	C=O
2951.4	2981.2	C_3–H
2975.4	3041.2	C_4–H

Carey *et al*. investigated similar compound, S-ethyl 4-hydroxybenzoate thioester. Their results of frequencies and shifts are in good agreement with our results with one exception. The C=O feature could not be detected because it is obscured by the ring modes or is vibrationally coupled with them. They observed two bands for the ring for the bound ligand and both showed sizable, 15–20 cm^{-1} downshifts when substrate was labeled with ^{13}C and ^{18}O in the benzoyl carbonyl group. It is likely that the normal mode structure of the two intense features is highly delocalized, encompassing the C=O bonds as well as the ring. Our calculation shows only one band for the ring: 1551.6 cm^{-1}. For the carbonyl group C=^{18}O we observed 10.5 cm^{-1} downshift. Carey *et al*. suggest that the ring becomes more quinonoid-like than benzenoid-like and concludes that the valence structure **1** (S-ethyl 4-hydroxybenzoate thioester) makes important contribution to the structure in the active site.

Our results demonstrate that the polarization is limited to the C_4=C_3–C_2=O_1 moiety. Thus ring appears unaffected upon binding to the enzyme and the canonical resonance structure **3** (DAC-CoA) makes important contribution to the ground state structure of the molecule. Our results are in good agreement with those observed by D'Ordine *et al*. [26,27]. They investigated 2,4-hexadienoyl-CoA using vibrational spectroscopy. They showed that the enzyme polarizes the ground state of the conjugated substrate analogs and this polarization is limited to the C_3=C_2–C_1=O portion of the acyl group. Thus, C_4=C_5 appears unaffected upon binding to the enzyme (structure **2**: 2,4-hexadienoyl-CoA).

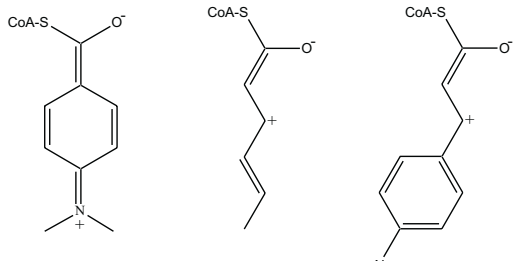

1 **2** **3**

Isotope substitution caused changes in frequencies. These changes are summarized in Table 6.

Table 6. Selected frequencies for substrate and product, ν (cm^{-1}).

	substrate in aqueous solution	substrate in the active site	enolate intermediate	product in the active site	product in aqueous solution
$C_2{=}^{16/18}O_1$	1913.8 (28.4)[a]	1923.7 (10.5)	1923.5 (6.5)	1938.0 (12.2)	1941.4 (40.8)
$C_3{=}^{12/13}C_4$	1827.6 (25.8)	1825.2 (7.2)	–	–	–
$C_2{=}^{12/13}C_3$	–	–	1923.5 (2.0)	–	–
$^{12/13}C_{3\alpha}$-H_{48}	–	–	–	2588.6 (3.6)	2922.2 (5.1)
$C_{3\alpha}{}^{1/2}H_{33}$	2951.4 (749.9)	2981.2 (433.6)	3078.7 (427.2)	2995.5 (225.8)	2922.2 (728.7)
$C_{4\beta}{}^{1/2}H_{34}$	2975.4 (759.2)	3041.2 (433.6)	2849.1 (426.8)	2903.7 (225.9)	2901.0 (762.1)

[a]Values in parentheses are shifts upon isotopic substitution by the heavy isotope indicated in the leading superscripts.

Table 7. Calculated isotope effects.

isotope effect	$^{13}C_3$	$^{13}C_4$	$^{2}H_{33}$	$^{2}H_{34}$	$^{18}O_1$
EIE_1[a]	0.9997	0.9990	0.9670	0.9195	0.9977
EIE_2[b]	1.0077	0.9957	0.9479	0.9546	0.9981
EIE_3[c]	1.0025	0.9999	1.0103	0.9646	1.0026
$EIE_1 \cdot EIE_2 \cdot EIE_3$[d]	1.0099	0.9946	0.9261	0.8467	0.9984

[a] – EIE on binding the reactant.
[b] – EIE on the chemical reaction in the active site pocket.
[c] – EIE on the release of the product.
[d] – overall EIE.

The carbonyl band corresponding to the bound substrate was compared to the free substrate in aqueous solution and showed that the band is shifted by 9.9 cm^{-1}. This shift is attributed to hydrogen bond formation between the DAC-CoA molecule and enzyme active site residues upon binding. One band 1923.7 cm^{-1} for $C_2{=}O_1$ is observed in case of the substrate in the active site (a result of the hydrogen bond formation). ^{18}O substitution caused 28.4 cm^{-1} shift in aqueous solution and 10.5 cm^{-1} in the active site.

We have computed $^{18}O_1$, $^{13}C_3$, $^{13}C_4$, $^{2}H_{33}$, $^{2}H_{34}$ equilibrium isotope effects. The values of these isotope effects are summarized in Table 7. ^{18}O equilibrium isotope effect on the enzyme-ligand association is capable of reflecting altered vibrational frequencies associated with hydrogen bond formation. The inverse value of this isotope effect indicates that the heavier isotope tends to concentrate in the enzyme-bound state and the C–O bond becomes stiffer when bound to the enzyme. The significant $^{2}H_{33}$ and $^{2}H_{34}$ isotope effects can be interpreted as resulting from the binding distortion. EIE's are strongly correlated with hydrogen bond lengths. This confirms that the hydrogen bond length can serve as a good indicator of hydrogen bond strength.

$$E + S \underset{k_{-1}}{\overset{k_1}{\rightleftarrows}} E \cdot S \underset{k_{-2}}{\overset{k_2}{\rightleftarrows}} E \cdot P \underset{k_{-3}}{\overset{k_3}{\rightleftarrows}} E + P \qquad (2)$$

where S – substrate, P – product, E·S – bound substrate, E·P – bound product.

We were able to use this approach in the case of the equilibrium ^2H isotope effect because the α and β deuterium equilibrium isotope effects for the dehydration of [(3S)-3-hydroxybutyryl]pantetheine by crotonase have been determined experimentally [2]. The value of $^2H_{33}$ EIE was found to be 1.07. From this value the EIE for the hydration direction can be evaluated as equal to 0.935 (1/1.07). Our calculations yield 0.926 ($EIE_1 \cdot EIE_2 \cdot EIE_3$). The measured value of the $^2H_{34}$ EIE is 1.33 for the dehydration corresponding to 0.752 for the hydration direction. Our calculation gives value equal to 0.847. These findings indicate that our model allows reliable prediction of the equilibrium isotope effects.

The oxygen $^{18}O_1$ isotope effect of binding to crotonase is small: 0.23%. This value indicates that hydrogen bonds are weak (the carbonyl oxygen is hydrogen bonded with Gly141 and Ala98, the length of that bond is 2.5 Å and 2.45 Å, respectively).

Acknowledgments

This work was supported by grants from the Maria Skłodowska-Curie Funds II and the Polish State Committee for Scientific Research. Computing time was provided by Cyfronet, Cracow, Poland.

REFERENCES

1. Willadsen P. and Eggerer H., *Eur. J. Biochem.*, **54**, 247 (1975).
2. Bahnson B.J. and Anderson V.E., *Biochem.,* **28**, 4173 (1989).
3. Bahnson B.J. and Anderson V.E., *Biochem.*, **30**, 5894 (1992).
4. Alston W.C., Haley K., Kanski R., Murray C.J. and Pranata J., *J. Am. Chem. Soc.*, **118**, 6562 (1996).
5. Alston W.C., Kanska M. and Murray C.J., *Biochem.*, **35**, 12873 (1996).
6. Stewart J.P.J., *J. Comp. Chem.,* **10**, 209 (1989).
7. Stewart J.P.J., *J. Comp. Chem.,* **10**, 221 (1989).
8. Jorgensen W.L., Chandrasekhas J., Madura J.D., Impey R.W. and Klein M.L., *J. Chem. Phys.*, **79**, 926 (1983).
9. HyperCube, Inc. Gainesville, Florida, USA.
10. Frisch M.J., Trucks G.W.,. Schlegel H.B, Scuseria G.E., Robb M.A., Cheeseman J.R., Zakrzewski V.G., Montgomery J.A., Stratmann Jr., R.E., Burant J.C., Dapprich S., Millam J.M., Daniels A.D., Kudin K.N., Strain M.C., Farkas O., Tomasi J., Barone V., Cossi M., Cammi R., Mennucci B., Pomelli C., Adamo C., Clifford S., Ochterski J., Petersson G.A., Ayala P.Y., Cui Q., Morokuma K., Malick D.K., Rabuck A.D., Raghavachari K., Foresman J.B., Cioslowski J., Ortiz J.V., Baboul A.G., Stefanov B.B., Liu G., Liashenko A., Piskorz P., Komaromi I., Gomperts R., Martin R.L., Fox D.J., Keith T., Al-Laham M.A, Peng C.Y., Nanayakkara A., Gonzalez C., Challacombe M., Gill P.M.W., Johnson B., Chen W., Wong M.W., Andres J.L., Gonzalez C., Head-Gordon M., Replogle E.S. and Pople J.A., Gaussian, Inc., Pittsburgh PA, 1998, Gaussian 98, Revision A.7.
11. Komaromi I., Dapprich S., Byun K.S., Morokuma K. and Frisch M.J., "A New ONIOM Implementation for the Calculation of Energies, Gradients and Higher Derivatives Using Mechanical and Electronic Embedding II." *Theo. Chem. Act.*, (1998).
12. Humbel S., Sieber S. and Morokuma K., *J. Chem. Phys*., **105**, 1959 (1996).
13. Maseras F. and Morokuma K., *J. Comp. Chem.*, **16**, 1170 (1995).

14. Matsubara T., Sieber S. and Morokuma K., *J. Quant. Chem.*, **60**, 1101 (1996).
15. Svensson M., Humbel S., Froese R.D.J., Matsubara T., Sieber S. and Morokuma K., *J. Phys. Chem.*, **100**, 19357 (1996).
16. Rappe A.K., Casewit C.J., Colwell K.S., Goddard W.A. III and Skiff W.M., *J. Am. Chem. Soc.*, **114**, 10024 (1992).
17. Rappe A.K. and Goddard W.A. III, *J. Phys. Chem.*, **95**, 3358 (1991).
18. Melaner L., Isotope Effects on Reaction Rates, Ronald Press, NY 1960.
19. Anisimov V. and Paneth P., *J. Math. Chem.*, **26**, 75 (1999).
20. Gawlita E., Paneth P. and Anderson V.E., *Biochem.*, **34**, 6050 (1995).
21. Gawlita E., Anderson V.E. and Paneth P., *Eur. Biophys. J.*, **23**, 353 (1994).
22. Sprang S., Standing T., Fletterick R.J., Stroud R.M., Finer-Moore J., Xuong N.H., Hamlin R., Rutter W.J. and Craik C.S., *Science*, 905 (1987).
23. Wilmouth R.C., Edman K., Neutze R., Wright P.A., Clifton I.J., Schneider T.R., Schofield C.J. and Hajdu J., *Nat. Struct. Biol.*, **8**, 689 (2001).
24. Li J., Zhu T., Cramer C.J. and Truhlar D.G., *J. Phys. Chem. A.*, **102**, 1820 (1998).
25. Dong J., Xiang H., Luo L., Dunaway-Mariano D. and Carey P.R., *Biochem.*, **38**, 4198 (1999).
26. D'Ordine R.L., Tonge P.J., Carey P.R. and Anderson V.E., *Biochem.*, **33**, 12635 (1994).
27. Tonge P.J., Anderson V.E., Fausto R., Kim M., Pusztai-Carey M. and Carey P.R., *Biospectr.*, **1**, 387 (1995).